Voltage Source Converter Control under Distorted Grid Voltage for Hybrid AC-DC Distribution Links

Wu, Y.; Shekhar, A.; Soeiro, T. B.; Bauer, P.

DOI
10.1109/IECON.2019.8927146

Publication date
2019

Document Version
Accepted author manuscript

Published in
Proceedings

Voltage Source Converter Control under Distorted Grid Voltage for Hybrid AC-DC Distribution Links

Yang Wu, Aditya Shekhar, Thiago Batista Soeiro and Pavol Bauer

***Abstract*—Back-To-Back (B2B) Voltage Source Converter (VSC) with AC-side LCL filters can be adopted for parallel AC-DC distribution links. In this paper, Grid-side Current Control (GCC) for the inner/fast control loops of the front- and back-end power electronics are implemented in order to enhance the system performance against grid disturbances. Herein, a notch filter-based GCC scheme with a harmonic rejection control is proposed which is able to deliver attenuation to the LCL filter resonances while suppressing the harmonics in the grid-side currents originated when the AC voltages are distorted. The results obtained in MATLAB/SIMULINK and an experimental prototype show that the studied GCC method can successfully mitigate the influence of grid voltage harmonics, while providing a stable power control for the hybrid AC-DC distribution links.**

***Index Terms*—Grid-side current control, notch filter, harmonic rejection, hybrid AC-DC distribution links.**

I. Introduction

Recent studies indicate that hybrid AC-DC distribution links as depicted in Fig.1 have a potential application in capacity enhancement and efficient power redirection under specific operating conditions, particularly for high power, medium voltage level and moderate distribution distances, e.g. 5....20 km, [1]–[4]. Back-To-Back (B2B) Voltage Source Converters (VSCs) with long DC buried cables in-between the transmitting- and receiving-end substations can be a feasible refurbishment strategy to such parallel AC-DC link architectures [5], [6].

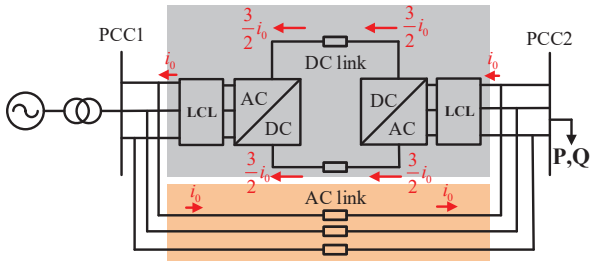

Fig. 1: Illustration of a hybrid AC-DC distribution link. A low impedance path for low frequency order zero-sequence current components is shown in-between the parallel system.

Different VSC topologies such as the conventional 2-level, 3-level Neutral-Point-Clamped (NPC) or Modular Multilevel Converters (MMC) have been employed for high power applications [7]. While MMCs have some performance advantages at medium voltage in such grid-connected applications [8], [9], e.g. better harmonic performance, the 2-level and 3-level VSCs have relatively lower operational complexity and cost as they typically employ less number of semiconductor switches. The later power electronic technologies can still achieve good current/voltage harmonic performance and compliance with the respective grid-connection requirements/standards by implementing high order passive AC filtering, such as the LCL filter configuration [12] and [13].

This paper focuses on the control challenges of operating VSCs with LCL passive filters under distorted grid voltage. Herein, for the fast/inner feedback control loop the direct measurement of the grid-side currents of the LCL filter has been chosen over the converter-side current measurement because a strict rejection of the undesirable effects created by the distorted grid voltages is desired. Generally, from the stability stand-point the choice of the controlled current side of the LCL filter, that is Grid-side Current Control (GCC) or Converter-side Current Control (CCC) depends on the relation between the resonance frequency, f_{res}, of the LCL filter and the critical frequency, f_{c}, which is defined by the sampling frequency of the digital control, f_{s}, where $f_{\text{c}} = \frac{1}{6} f_{\text{s}}$ [10]–[12]. Specifically, according to [10], CCC is preferred if f_{res} is smaller than f_{c}. On the other hand, GCC is recommended if f_{res} lies between f_{c} and $\frac{1}{2} f_{\text{s}}$ [10], [11]. Therefore, a robust-oriented design of the LCL filter have the resonance frequency located within the assigned stable region according to the employed feedback digital control scheme.

Note that even when the LCL resonance frequency falls in an unstable region for the GCC or CCC schemes, stable current feedback control can be achieved by other additional means, e.g. addition of an external circuit able to suppress any AC voltage or current resonances. For example, passive circuit damping has a satisfactory performance with the trade-off of extra power loss [14]. Active Damping (AD) methods have been widely investigated and they can effectively solve the resonance influence at the cost of reduced control bandwidth [15]. Virtual resistor and notch filter-based active damping are the two most used AD methods. For implementing virtual resistors the control loop typically requires the information/measurement of the filter capacitor voltage (or current). This information is used in an equivalent feed-forward control loop to mimic the effects of a damping resistor seen by the capacitor voltage.

Notch filter can realize effective damping while maintaining a single current measurement for the feedback control

loop [16]. Design guidelines for this solution has been proposed in [16]–[18], where the depth and width of the notch filter are set as a trade-off to minimizes its influence on the open loop gain of the current control in the low frequency region.

Grid voltage feed-forward can not effectively mitigate the influence from its voltage distortions and a Harmonics Rejection (HR) controller is required in order to realize power delivery with satisfactory current waveform and power ripples [19]. In this paper, a notch filter-based resonance damping and low order harmonic rejection controls are combined in the grid-side current control scheme to increase the robustness against the grid disturbances while preventing instability created by the resonance of the LCL filter. The paper tests the highlighted control concepts both through simulations and experiments using a single VSC connected to a distorted grid voltage with the future goal of realizing the same in a parallel AC-DC link system.

The paper is structured as follows: Section II presents the description of the parallel AC-DC link and suitable feedback control scheme. The analysis of a Notch filter damping and harmonic controls are shown in Section III. Simulation results are given in Section IV and the experimental results are shown in Section V. Conclusion and future work are presented in Section VI.

II. System Description

A. Parallel AC-DC Operation

Parallel AC-DC re-configurable link system can implement purely DC, AC and hybrid AC-DC power delivery. Parallel AC-DC operation (as depicted in Fig.1) is a special configuration [4]. In this operation, the main grid delivers power to loads (P and Q) in part by both AC and DC links using the power steering capability of the B2B system. The AC/DC converter is responsible to control and build-up the DC-link voltage while the DC/AC converter is responsible to control/inject the required active and reactive powers demanded by the loads. In such operating conditions, current distortions in the DC/AC converter will flow through the AC link in parallel, thus resulting in additional losses.

For example, it was shown in [22] that although the system constitutes a three-wire point-to-point configuration a low impedance path for the Zero Sequence Circulating Currents (ZSCC) exists between the two parallel AC and DC links. The path of these currents are shown in Fig. 1. As it can be notice the AC filtering inductances and cable impedances are the main elements limiting the ZSCC.

Additionally under distorted grid voltage the capacitor of the LCL filter acts as a sink to harmonic currents. While GCC can reject these currents from flowing via the parallel AC link, it could be that the necessary bandwidth is restricted by the resonant frequency of the LCL filter. The paper deals with this specific issue using an active damping method.

B. Vector Control in Rotating Frame

Fig. 2 shows the control diagram for the VSC. An outer control loop is used to either regulate the DC-link voltage (rectifier) or control the active power (inverter). A fast/inner controller controls the corresponding grid-side currents (Section II-C). The grid synchronization information is obtained by means of a Phase-Lock-Loop (PLL). The control method presented in this paper is realized in dq0 frame.

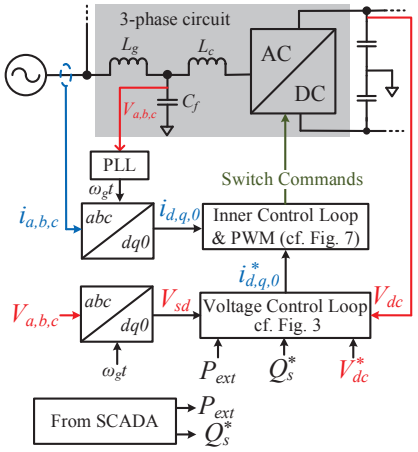

Fig. 2: Control Diagram for both AC/DC and DC/AC converters.

1) Power Control: In dq-frame, the active and reactive power are proportional to d- and q-axis components of the grid current respectively as described by eqs. (1) and (2).

$$i^*_{\mathrm{d}} = \frac{2}{3V_{\mathrm{sd}}} P^*_{\mathrm{s}} \tag{1}$$

$$i^*_{\mathrm{q}} = -\frac{2}{3V_{\mathrm{sd}}} Q^*_{\mathrm{s}} \tag{2}$$

Where V_{sd} is the d-axis component of the grid voltage.

2) DC Link Voltage Control: The block diagram for the voltage controller cascaded with the composite control plant [24] is shown in Fig. 3.

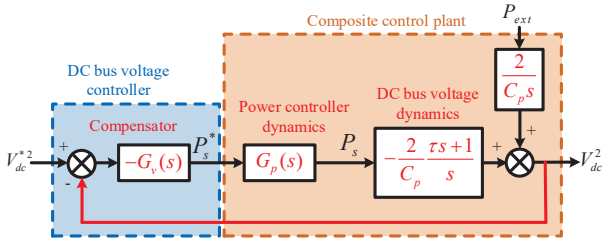

Fig. 3: DC bus voltage control diagram.

The voltage controller regulates V^2_{dc} and generates the active power reference through the PI control based compensator

$G_v(s)$. τ is the time constant of the DC bus dynamics which is proportional to the product of AC side inductance of the VSC and the steady-state real power flow [24].

C. Grid-current Control of VSC filtered by LCL

Fig.4 presents the GCC block diagram, where $G_c(s)$ is the current controller given by (3) and $G_f(s)$ is the feed-forward control of the grid voltage.

$$G_c(s) = k_p + \frac{k_i}{s} \tag{3}$$

$G_d(s) = e^{-sT}$ represents the digital controller delay due to sampling, where T is the digital control delay time with one-sample delay (i.e., $T = T_s = \frac{1}{f_s}$), which is applicable for typical digital implementations [7]. $G_{inv}(s)$ is the combined Transfer Function (TF) of the PWM modulator and respective digital sampling and delay. PWM delay is approximately modelled as a zero-order-holder (ZOH) and G_{inv} can be mathematically derived by eq. (4) if synchronous PWM sampling is considered [20],

$$G_{inv}(s) = \frac{1}{T_s}\frac{1 - e^{-sT_s}}{s} k_{pwm} \approx k_{pwm} e^{-0.5sT_s} \tag{4}$$

where k_{pwm} is the ratio between DC voltage and the amplitude of the triangular carrier.

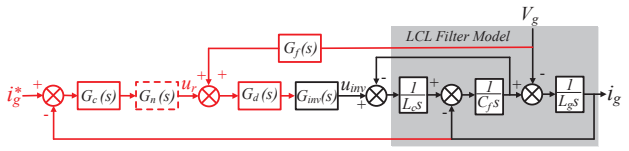

Fig. 4: Current control model of grid-connected VSC with LCL Filter.

The TF from the converter output voltage u_{inv} to the grid side current i_g and converter-side current i_c can be derived as (5) from the LCL filter model shown in Fig.2.

$$\begin{aligned} G^{ig}_{u_{inv}}(s) &= \frac{1}{sL_cL_gC_f}\frac{1}{s^2+\omega_{res}^2} \\ G^{ic}_{u_{inv}}(s) &= \frac{s^2L_cC_f+1}{sL_cL_gC_f}\frac{1}{s^2+\omega_{res}^2} \end{aligned} \tag{5}$$

where the resonance frequency is derived as:

$$\omega_{res} = \sqrt{\frac{L_c + L_g}{L_cL_gC_f}} \tag{6}$$

III. Notch Filter Based GCC with Harmonic Control

A. Grid-side current Control with Notch Filter

To solve the LCL resonance problem when f_{res} falls into the unstable region for the GCC scheme, a notch filter was recommended by [14] to provide required attenuation at corresponding frequency range. The notch filter $G_n(s)$ is added in the control loop as shown in Fig. 4. According to [19], the TF from converter voltage to grid side current with the damping ratio ζ is given by (7).

$$G^{ig}_{u_{inv\_d}}(s) = \frac{1}{sL_cL_gC_f}\frac{1}{s^2+2\zeta\omega_{res}s+\omega_{res}^2} \tag{7}$$

The corresponding notch filter TF can be derived by dividing eq. (7) by eq. (5) and is given by (8),

$$G_n(s) = \frac{G^{ig}_{u_{inv\_d}}(s)}{G^{ig}_{u_{inv}}(s)} = \frac{s^2+\omega_{res}^2}{s^2+2\zeta\omega_{res}s+\omega_{res}^2} \tag{8}$$

The TF from (8) is modified to (9) to take into account the damping provided by the internal resistances of the various VSC system components.

$$G_n'(s) = \frac{s^2+2\zeta_z\omega_{res}s+\omega_{res}^2}{s^2+2\zeta_p\omega_{res}s+\omega_{res}^2} \tag{9}$$

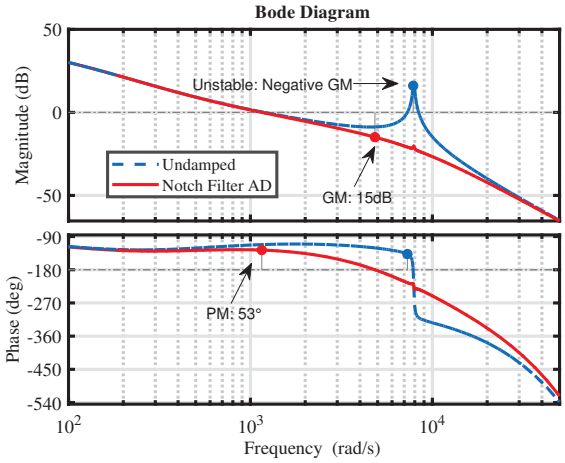

Fig. 5: Open loop bode plot of GCC with notch filter AD.

Herein, ζ_z and ζ_p are the damping factors that can be determined based on the design requirements, i.e.,attenuation and width of the notch filter as discussed in [12]. Fig. 5 shows the open loop bode plot of the current control with and without notch filter. Therein, the LCL parameters are given as $L_c = 1.5\,\text{mH}$, $L_g = 1.5\,\text{mH}$ and $C_f = 20\,\mu\text{F}$ based on the parameters of the two available 5 kVA lab-scale VSCs which will be used in this paper to verify the study developed here [25]. In order to model the effects of the AC filter inductor and semiconductor losses of the VSC an equivalent resistor is added in series with each inductor. This resistor is assumed to be $0.2\,\Omega$ and it is back calculated based on the measured efficiency of the VSC. Herein, the PWM sampling frequency is 16 kHz. $k_p = 3.5$ and $k_i = 1600$ are selected for control according to the frequency-response method, which is also called loop shaping. Without any damping, the current loop is unstable according to Nyquist Stability Criterion as a negative Gain Margin (GM) is observed. With the notch filter active damping ($\zeta_p = 0.9$, $\zeta_z = 0.01$), positive GM of 15 dB and Phase Margin (PM) of 53° are provided. The stability is achieved by sacrificing the control bandwidth as

the gain in the frequency range corresponding to the notch filter decreases. Stability can also be improved without using a notch filter if smaller loop gain is chosen. However, this method results in relatively greater reduction in bandwidth of the current controller as the smaller gain corresponds to the entire frequency spectrum.

B. Harmonics Rejection Control

1) Grid Impedance Analysis: The distorted grid voltage V_{g} can be regarded as a disturbance term as depicted in Fig. 4. This distortion can influence the grid current quality because the capacitor of the LCL filter acts as a high-frequency sink for these harmonics. This is specifically undesirable because the resulting harmonic currents will flow through the AC link in parallel, leading to additional losses. Therefore, a resonator-based harmonics controller is adopted based on the harmonics impedance shaping method discussed in [19], [20]. The control output for the GCC is given by (10),

$$i_{\mathrm{g}} = i_{\mathrm{ref}} \frac{G(s)G^{\mathrm{ig}}_{u_{\mathrm{inv}}}(s)}{1+G(s)G^{\mathrm{ig}}_{u_{\mathrm{inv}}}(s)} + V_{\mathrm{g}} \frac{G_{\mathrm{F}}(s) - G^{\mathrm{ic}}_{u_{\mathrm{inv}}}(s)}{1+G(s)G^{\mathrm{ig}}_{u_{\mathrm{inv}}}} \tag{10}$$

where $G(s) = G_{\mathrm{c}}(s)G_{\mathrm{notch}}G_{\mathrm{d}}(s)G_{\mathrm{inv}}(s)$ and $G_{\mathrm{F}}(s)$ represents $G_{\mathrm{f}}(s)G_{\mathrm{d}}(s)G_{\mathrm{inv}}(s)$. The TF of the equivalent grid impedance is given by (11),

$$Z_{\mathrm{g}}(s) = \frac{1+G(s)G^{\mathrm{ig}}_{u_{\mathrm{inv}}}(s)}{G_{\mathrm{F}}(s) - G^{\mathrm{ic}}_{u_{\mathrm{inv}}}(s)} \tag{11}$$

The filter-related admittance TF are fixed once the LCL parameters are selected. However, resonators can be added to the current controller to shape the grid impedance TF.

In stationary ($\alpha\beta$) frame, PR (Proportional Resonant) is used for tracking the sinusoidal reference at fundamental frequency. Adding harmonic resonators (HR) in parallel with the PR compensator will not affect the reference tracking capability and can effectively increase those harmonic impedances, as shown in Fig. 6.

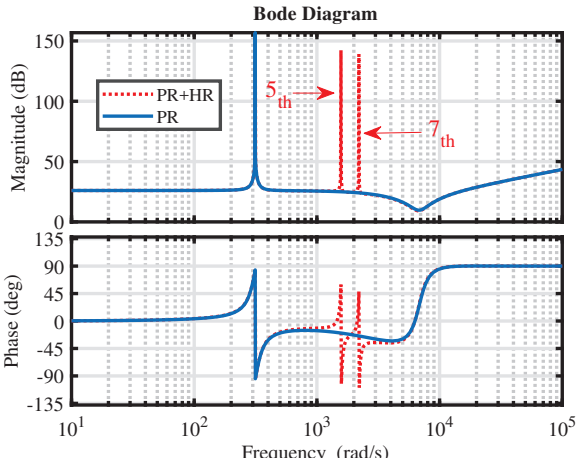

Fig. 6: Bode plot of Z_g with PR and PR+HR controller

The TF of PR + HR controller are given by (12),

$$G_{\mathrm{PR+HR}}(s) = \underbrace{k_{\mathrm{p}} + \frac{k_{\mathrm{r}}s}{s^2+\omega^2}}_{\mathrm{PR}} + \underbrace{\sum_{h=1,2,3\cdots}^{\infty} \frac{k_{\mathrm{h}}s}{s^2+\omega_{\mathrm{h}}^2}}_{\mathrm{HR}} \tag{12}$$

where ω_{h} is the frequency of the harmonics to be eliminated (for example, 5_{th} and 7_{th} harmonics are depicted in Fig. 6).

2) Harmonics Controller in dq Frame: The positive and negative sequence harmonic frequencies are expressed by (13) and (14),

$$\begin{cases} \omega_{+} = (3n+1)\omega t, & n = 1,2,3\cdots \end{cases} \tag{13}$$

$$\begin{cases} \omega_{-} = -(3n-1)\omega t, & n = 1,2,3\cdots \end{cases} \tag{14}$$

After one fundamental frequency unit shift, the frequency in dq frame becomes:

$$\begin{cases} \omega_{dq+} = 3n\omega t, & n = 1,2,3\cdots \end{cases} \tag{15}$$

$$\begin{cases} \omega_{dq-} = -3n\omega t, & n = 1,2,3\cdots \end{cases} \tag{16}$$

Therefore, one resonator in dq frame is used to reject adjacent positive and negative-sequence harmonics. as shown in Fig. 7.

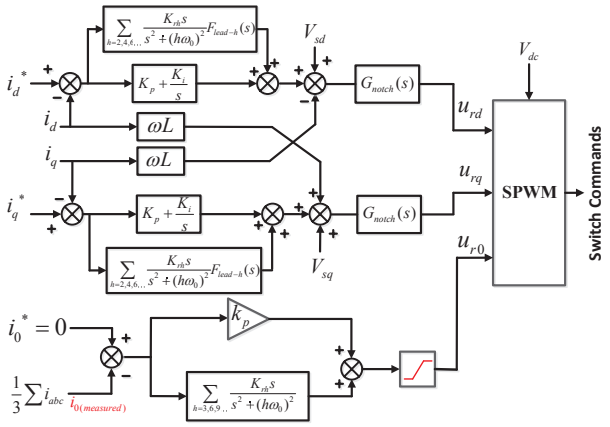

Fig. 7: Current controller structure with PI + HR in dq frame

Sinusoidal PWM (SPWM) instead of Space-Vector Pulse-width Modulation (SVPWM) is chosen because the latter will introduce zero-sequence terms to the modulated voltage [21]. A method to mitigate the resulting ZSCC in hybrid AC/DC distribution links is discussed in [22].

3) Phase Margin Improvement with Lead Filter: The implementation of the harmonics resonators increases the harmonics impedance at the cost of phase margin detriment around the selected frequency. To improve phase margin, the loop gain has to be sacrificed. Lead filter is a good phase compensation option as it can provide a maximum of 90° increase at an specific frequency while zero-compensation can only provide a maximum of 45° phase increment [14]. To avoid the gain decrease below the selected frequency, the lead filter is connected directly to the resonator. Each resonator has its

corresponding lead filter, which provides phase increase at the selected frequency.

IV. Simulation Results

The system parameters used for the presented simulation results are listed in Table. I.

TABLE I: System Parameters for Simulation

Parameter	Value
L_g=L_c	1.5 mH
C_f , C_{dc}	20 μF , 600 μF
R_{link}	0.5 Ω
$V_{s_{rms}}$ V_{dc}	230 V , 1 kV
f_m , f_{sw} , f_s	50 Hz , 16 kHz , 16 kHz
P_{ac} , P_{dc} , P_{load}	5 kW , 5 kW , 10 kW
Q_{ac} , Q_{dc} , Q_{load}	0 VAR , 0 VAR , 0 VAR
k_p , k_i , k_{rh}	3.5 , 1600 , 8000

R_{link} is the resistance of single conductor, with AC link having three conductors while DC link having two conductors. P_{ac}, P_{dc} are the active power and Q_{ac}, Q_{dc} are the reactive powers of the AC and DC links. The simulation results test the operation of a single VSC delivering 5 kW DC load while connected to a distorted ac grid voltage with 2% 5_{th} and 7_{th} harmonics. The stability of the grid current control with notch filter is firstly verified, as shown in Fig. 8. It can be observed that the system becomes unstable when the notch filter is disabled at 0.8 s.

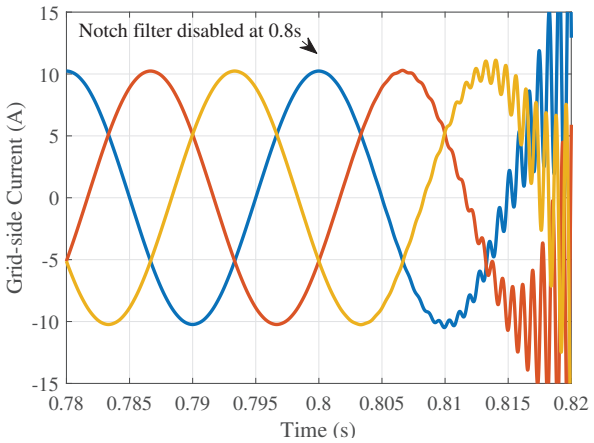

Fig. 8: Power control of the VSC at $P_{ref} = 5kW$(PI+Notch).

Fig. 9 shows the performance of the harmonics controller. Grid current Total Harmonic Distortion (THD) is reduced from 13.31% to 0.48%, which is close to the THD of the grid-side current (0.3%) under ideal/purely sinusoidal 50 Hz grid voltage.

V. Experimental Validation

The VSC shown in Fig. 10 works as a STATCOM and delivers reactive power to a grid. Fig. 11 shows the results when the converter delivers 1.5 kVAR with purely sinusoidal

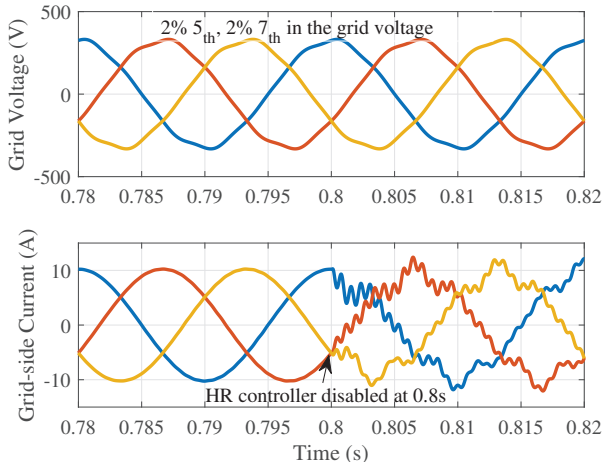

Fig. 9: Power control of the VSC at $P_{ref} = 5kW$ (PI+HR+Notch)

50 Hz grid voltage. The THD in the measured grid-side current is 1.4%. Fig. 12 shows the measured converter output current

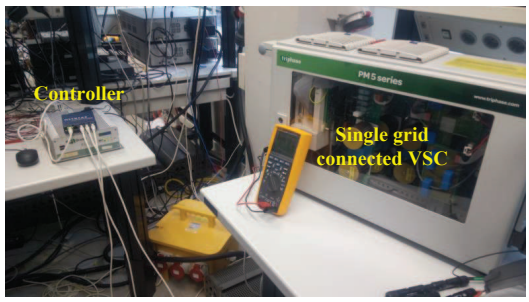

Fig. 10: Experimental setup showing a single grid connected VSC operating as a STATCOM under distorted voltage

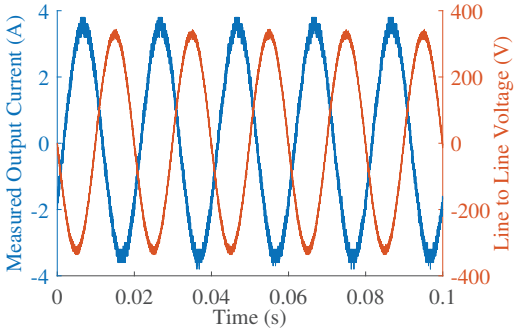

Fig. 11: Measured wave-forms with purely sinusoidal 50 Hz grid voltage.

wave-forms with and without HR control under distorted grid voltage. The 5_{th} and 7_{th} harmonics in the grid-side current reduced from 15.7% and 6.7% to 2% and 1.9% respectively after the harmonics resonators are implemented in the control.

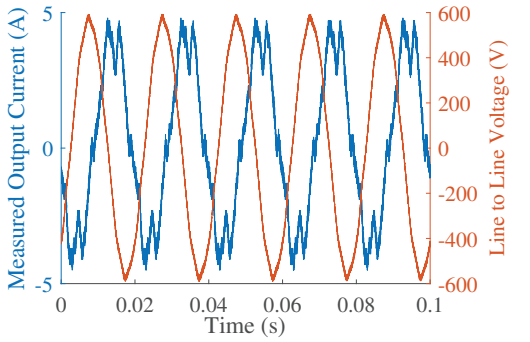

(a) Without HR control.

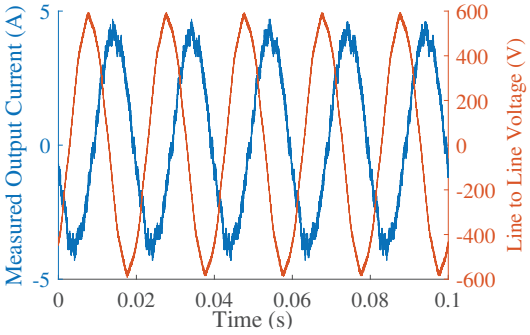

(b) With HR control.

Fig. 12: Measured converter output currents under distorted grid voltage.

The total harmonic distortion (THD) for the grid-side current is reduced from 18.86% to 7.3%.

VI. Conclusion and Future Work

A grid side current controller with notch filter and harmonics resonator is proposed in this paper to implement stable power control in hybrid AC-DC distribution links under distorted grid voltage conditions. Simulation results show that the proposed controller (PI+Notch+HR) can effectively mitigate the harmonics components in the grid current and reduce the power ripples under grid distortion while maintaining stability from the LCL filter resonance. With precise power control in hybrid AC-DC links, the VSCs adjust the currents in the AC links by controlling the power injected to the load through the DC distribution path. As future work, the control scheme will be implemented experimentally in a parallel ac-dc link system to demonstrate its working along with ZSCC control.

References

[1] S. I. Nanou and S. A. Papathanassiou, "Frequency Control of Island VSC-HVDC Links Operating in Parallel With AC Interconnectors and Onsite Generation," in *IEEE Transactions on Power Delivery,* vol. 33, no. 1, pp. 447-454, Feb. 2018.

[2] T. Joseph, J. Liang, G. Li, A. Moon, K. Smith and J. Yu, "Dynamic control of MVDC link embedded in distribution network: Case study on ANGLE-DC," *IEEE Conference on Energy Internet and Energy System Integration (EI2),* Beijing, 2017, pp. 1-6.

[3] S. K. Chaudhary, J. M. Guerrero and R. Teodorescu, "Enhancing the Capacity of the AC Distribution System Using DC InterlinksA Step Toward Future DC Grid," in *IEEE Transactions on Smart Grid,* vol. 6, no. 4, pp. 1722-1729, July 2015.

[4] A. Shekhar, L. Ramrez-Elizondo, T. B. Soeiro, and P. Bauer, "Boundaries of operation for refurbished parallel ac-dc reconfigurable links in distribution grids," *IEEE Trans. Power Del.*, pp. 1-1 May. 2019.

[5] L. Zhang, J. Liang, W. Tang, G. Li, Y. Cai and W. Sheng, "Converting AC Distribution Lines to DC to Increase Transfer Capacities and DG Penetration," in *IEEE Transactions on Smart Grid,* vol. 10, no. 2, pp. 1477-1487, March 2019.

[6] D. M. Larruskain, I. Zamora, O. Abarrategui, A. Iturregi, "VSC-HVDC configurations for converting AC distribution lines into DC lines," *International Journal of Electrical Power Energy Systems,* Volume 54, 2014, Pages 589-597.

[7] A. Laka, J. A. Barrena, J. Chivite-Zabalza, M. . Rodrguez Vidal and P. Izurza-Moreno, "Voltage Source Converter Topology for High-Power Applications Serializing Three-Phase Converters and H-Bridges," *IEEE Trans. Ind. Electron.*, vol. 61, no. 10, pp. 5184-5191, Oct. 2014.

[8] J. E. Huber and J. W. Kolar, "Optimum Number of Cascaded Cells for High-Power Medium-Voltage ACDC Converters," in *IEEE Journal of Emerging and Selected Topics in Power Electronics,* vol. 5, no. 1, pp. 213-232, March 2017.

[9] A. Shekhar, L. B. Larumbe, T. B. Soeiro, Y. Wu and P. Bauer, "Number of Levels, Arm Inductance and Modulation Trade-offs for High Power Medium Voltage Grid-Connected Modular Multilevel Converters," *ICPE-ECCE Asia IEEE,* Busan, South Korea, 2019.

[10] C. Zou, B. Liu, S. Duan and R. Li, "Influence of Delay on System Stability and Delay Optimization of Grid-Connected Inverters With LCL Filter," *IEEE Trans.Ind. Inf.*, vol. 10, no. 3, pp. 1775-1784, Aug. 2014.

[11] J. Wang, J. D. Yan, L. Jiang and J. Zou, "Delay-Dependent Stability of Single-Loop Controlled Grid-Connected Inverters with LCL Filters," *IEEE Trans. Power Electron.*, vol. 31, no. 1, pp. 743-757, Jan. 2016.

[12] J. Yin, S. Duan and B. Liu, "Stability Analysis of Grid-Connected Inverter With LCL Filter Adopting a Digital Single-Loop Controller With Inherent Damping Characteristic," *IEEE Trans.Ind. Inf.*, vol. 9, no. 2, pp. 1104-1112, May 2013.

[13] M. Lindgren and J. Svensson, "Control of a voltage-source converter connected to the grid through an LCL-filter-application to active filtering," *in Proc. Power Electron. . Specialists Conf*, vol. 1, pp. 229-235, April. 1998.

[14] J. Dannehl, M. Liserre and F. W. Fuchs, "Filter-Based Active Damping of Voltage Source Converters WithLCLFilter," *IEEE Trans. Ind. Electron.*, vol. 58, no. 8, pp. 3623-3633, Aug. 2011.

[15] M. A. Gaafar and M. Shoyama, "Active damping for grid-connected LCL filter based on optimum controller design using injected grid current feedback only," in *IEEE ECCE*, pp. 3628-3633, Sept.2014

[16] W. Yao, Y. Yang, X. Zhang and F. Blaabjerg, "Digital notch filter based active damping for LCL filters," in *Proc. of IEEE APEC*, pp. 2399 -2406, 2015

[17] R. Pea-Alzola, M. Liserre, F. Blaabjerg, M. Ordonez and T. Kerekes, "A Self-commissioning Notch Filter for Active Damping in a Three-Phase LCL -Filter-Based Grid-Tie Converter," *IEEE Trans. Power Electron.*, vol. 29, no. 12, pp. 6754-6761, Dec. 2014.

[18] P. Channegowda and V. John, "Filter Optimization for Grid Interactive Voltage Source Inverters," *IEEE Trans. Ind. Electron.*, vol. 57, no. 12, pp. 4106-4114, Dec. 2010.

[19] Y. Jia, J. Zhao and X. Fu, "Direct Grid Current Control of LCL-Filtered Grid-Connected Inverter Mitigating Grid Voltage Disturbance," *IEEE Trans. Power Electron.*, vol. 29, no. 3, pp. 1532-1541, March 2014.

[20] P. Sung-Yeul, C. Chen, L. Jih-Sheng, and M. Seung-Ryul, Admittance compensation in current loop control for a grid-tie LCL fuel cell inverter, *IEEE Trans. Power Electron.*, vol. 23, no. 4, pp. 17161723, Jul. 2008.

[21] T. Chen, Zero-Sequence Circulating Current Reduction Method for Parallel HEPWM Inverters Between AC Bus and DC Bus, *IEEE Trans. Ind. Electron.*, vol. 59, no. 1, pp. 290-300, Jan. 2012.

[22] A. Shekhar, T. B. Soeiro, L. Ramrez-Elizondo, and P. Bauer, Zero Sequence Currents Externally Circulating between the Back to Back Modular Multilevel Converters in Parallel AC-DC Distribution Links, *2019 IEEE ECCE Asia Busan,* Korea 2019.

[23] C. Pan and Y. Liao, "Modeling and Coordinate Control of Circulating Currents in Parallel Three-Phase Boost Rectifiers," *IEEE Trans. Power Electron.*, vol. 54, no. 2, pp. 825-838, April. 2007.

[24] Y. Amirnaser and Iravani, R *Voltage - sourced converters in power systems: modeling, control, and applications*. New Jersey: IEEE Press, 2012.

[25] R. T. Pinto, "System integration, dynamics and control, in Multi-terminal DC Networks," Phd Thesis, *Delft University of Technology,* 2013.